Special Report 28
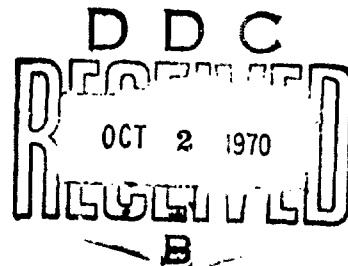
JULY, 195.

Measurements of Ice Tunnel Deformation Camp Red Rock, Greenland

by Robert E. Hilty

D D C

OCT 2 1970

B

U. S. ARMY SNOW ICE AND PERMAFROST
RESEARCH ESTABLISHMENT
Corps of Engineers
Wilmette, Illinois

This document has been approved
for public release and sale; its
distribution is unlimited.

Best
Available
Copy

PREFACE

This is a report of work performed during the 1957 Greenland field season on USA SIPRE Project 22.1-24 and CE Project 24, Ice cliff studies. The purpose of these investigations was to obtain basic information regarding ice motion, recent history of the ice edge, and the physical characteristics of the ice, as a basis for further engineering research. Part of the work was performed under Contract DA-11-190-ENG-19 with Ohio State University.

The research work was performed by Mr. Robert E. Hilty.* Work on this project was performed for the Snow and Ice Basic Research Branch, Mr. James A. Bender, chief.

WALTER H. PARSONS, JR.
Colonel, Corps of Engineers
Director

Manuscript received 12 February 1958
Department of the Army Project 8-66-02-400

*Standard Oil Company of Texas, San Antonio, Texas

CONTENTS

ILLUSTRATIONS

TABLES

ICE TUNNEL DEFORMATION MEASUREMENTS

CAMP RED ROCK, GREENLAND

by

Robert E. Hilt

INTRODUCTION

Detailed scientific studies on the regimen of the cliff terminus of the North Ice Cap in Greenland were initiated as a full scale project (CE Project 24) in the summer of 1955, at Camp Red Rock, Nunatarssuaq, 40 miles northeast of Thule Air Base. One of the several means of gathering information was through deformation studies in a 30-m deep horizontal tunnel excavated normal to the trend of the cliff face and aligned essentially parallel to the direction of glacier flow. During the spring and summer of 1956, a tunnel addition (referred to here as the 1956 tunnel) was extended from the side of the 1955 tunnel. The excavation in 1956 was dug to a lower level and exposed approximately 15 m^2 of bouldery subglacial floor. This provided an excellent opportunity to obtain precise and detailed information on basal glacier movement as well as to study the effects on a patch of frozen ground suddenly relieved of high stresses. The tunnel walls and ceiling were instrumented with several rings of motion pegs which were surveyed with a theodolite from a system of stationary stakes. Mapping of the ice stratigraphy and other deformation studies augmented the motion survey.

The primary objective of Project 24 in 1957 was to resurvey the position of the pegs in the 1956 tunnel. Compilation of data and conclusions derived constitute the basis of this report.

EXCAVATION

The 1956 section of tunnel was begun in order to expose the downward traces of heavily dirt-laden shear planes, prominent in the 10-m area of the 1955 tunnel, and to discover their configuration and the nature of bottom contact (Fig. 1 - 2).

Figure 1. Looking south in tunnel, August 1956.

Figure 2. Looking south in tunnel, June 195?. Notice bowed-in west wall and bouldery floor.
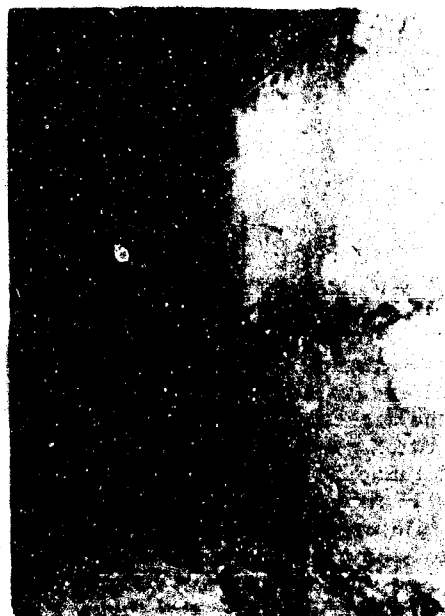
Figure 3.   Dirt layers in west wall
near ring 4.

Figure 4.   "Suspended" dirt layers on west
wall near ring 3.   Note sand and ice floor
on left and boulder floor on right.

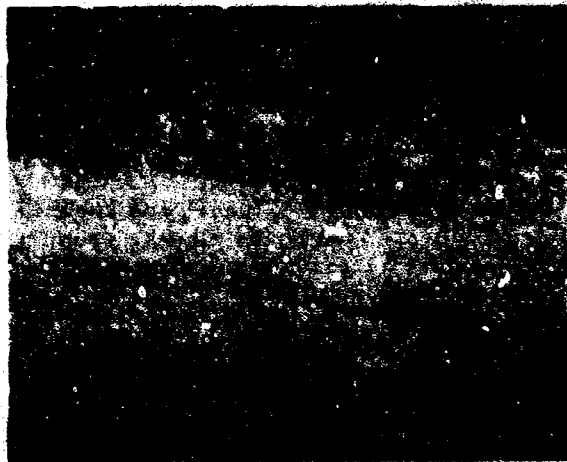Figure 5.   Ice stratigraphy and interbedded
dirt bands, on west wall 2 m south of ring 4.

The extension started perpendicular
from the east wall at about 9 m in from
the mouth of the 1955 tunnel.   The shaft
gradually curved to a northerly direction
and descended steeply in an attempt to
remain in the plane of the waning dirty
ice bands.   The principal portion of the
1956 excavation extended 15 m northward
from the descending curve and was
orientated essentially parallel to the 1955
tunnel (Fig. 6).   The rocky floor of the
tunnel sloped slightly northward about
70 cm over the 15-m length.   The height
of the tunnel decreased from 5 m above
the floor at the south end to 2 m above it
at the north end.

STRATIGRAPHY

The shear planes of the 1955 excavation terminated abruptly, shortly below the
1955 tunnel level.   However, another set of dirt layers, not connected to those
mentioned above, were interbedded in the ice at the south end of the tunnel (Fig. 3-
5, 7).   These dirt bands consisted of solid pebbly sand ranging from a few
centimeters in thickness throughout most of the layer to a maximum of 20 cm in the
irregularly spaced pods.   The dirt layers dipped northward in the same direction as
the ice foliation.   Ice-dirt contact was always sharp and conformable to slightly non-
conformable.   No folding was apparent in the dirt bands.   The ice varied from green
to white to gray and dipped approximately 7°N at the north end of the tunnel and up to
23°N at the south end nearer the ice terminus.   Original dips taken on the dirt bands
and ice foliation were remeasured in 1957 and no appreciable differences could be
detected.

Lichen-covered boulders up to 1 m in diameter constituted most of the tunnel
floor (Fig. 2).   A smaller area in the southern portion was covered with a thick
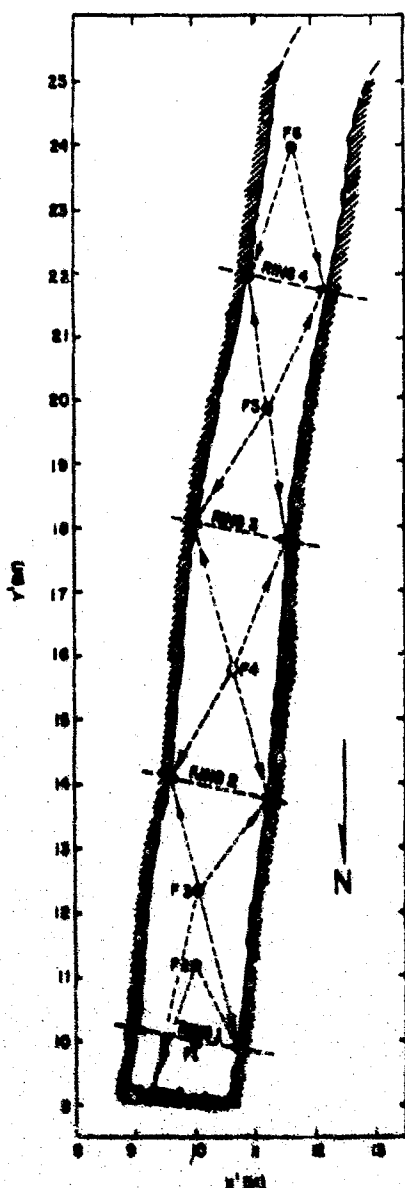blanket of interbedded sand and ice layers (Fig. 4).

Figure 6. Diagram of 1956 tunnel show-
ing rings of pegs and triangulation
network in relation to coordinate system.

It is postulated that the ice and dirt
sequence exposed on the walls of the 1956
tunnel formed from a snow drift over-
ridden by and incorporated in the
advancing North Ice Cap. Facts support-
ing this hypothesis are: a) the highly
folded dirt bands in the 1955 tunnel did not
reach the basal part of the glacier; b) the
dirt bands in the 1956 tunnel were unfolded,
had a low dip, and appeared to be
depositional rather than tectonic features;
c) these suspended dirt layers appeared to
have had no former connection with the
subglacier terrain. In a plunge pool 140 m
west of the tunnel and at the base of the
cliff, a very similar stratigraphic section
was observed in a snow drift which extend-
ed directly under the ice cliff.

Not only did the tunnel cut provide an
excellent exposure of basal ice stratigraphy,
but the stable floor furnished the possibility
of an internal baseline for precise defor-
mation studies under approximately 40 m
of ice and under uniform temperature
conditions on the order of -10C.

INSTRUMENTATION

Four rings of pegs were set in the walls
at 4-m intervals; crossed rows of pegs
were lined along the back face, and
auxiliary pegs were placed at the south end
of the west wall (Fig. 7). Because of lack
of time, only a majority of the ring pegs
and the back face pegs were resurveyed.
Plumb and tape measurements were taken
on the auxiliary pegs. Absolute motion was
triangulated on 55 pegs in mid-August 1956
and again in early June 1957. The time
interval amounted to an average of 294 days.

Pegs consisted of 15 cm long by 1 cm
diam wooden dowels soaked in water and
forced into a hole of the same diameter.
Steel pins driven into the ends of the dowels
were clipped to a point to provide a sharp
target. The floor pegs employed as
triangulation stations were 2.5 cm diam steel
rods driven securely between the boulders.

A Wild T-2 theodolite was used to triangulate each peg from two floor stations
(Fig. 6). The single set of direct and reverse angles taken were within 30 sec
difference with very few exceptions and usually within 10 sec difference. Considering
this amount of variation over the short distances used, the peg coordinates presented
are accurate to the nearest centimeter. Rough plumb and tape measurements on the
west wall of rings 1 and 4 check within 5% of those obtained by triangulation.

The only case where the triangulated peg positions are beyond reasonable accuracy
is on the back face. Angles from both stations were in the range of 180° and the
resulting discrepancies in the peg coordinates render them unreliable.

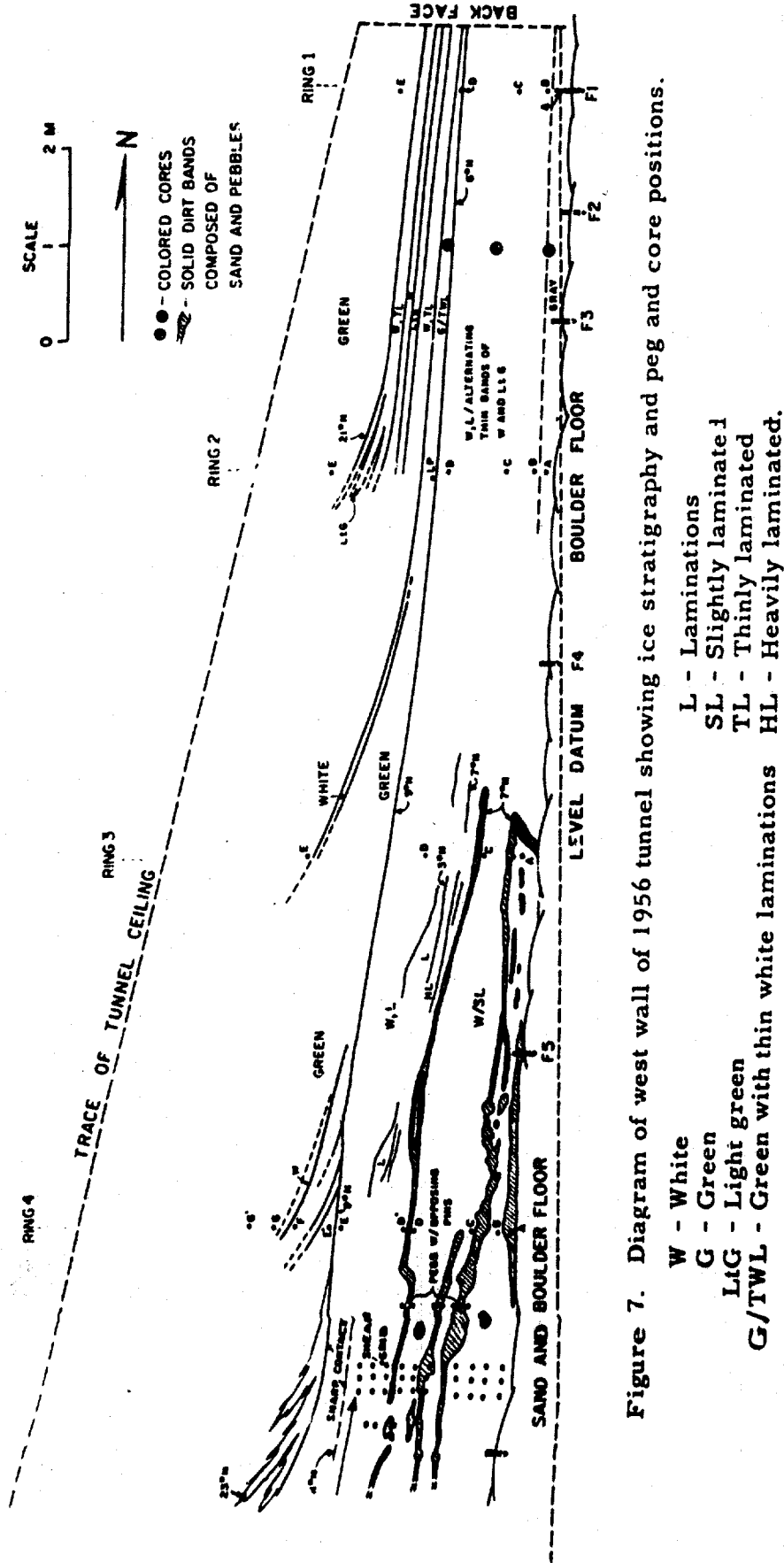Figure 7. Diagram of west wall of 1956 tunnel showing ice stratigraphy and peg and core positions.

W – White
G – Green
LtG – Light green
G/TWL – Green with thin white laminations

L – Laminations
SL – Slightly laminated
TL – Thinly laminated
HL – Heavily laminated.

It is evident that the floor did not respond to the removal of the ice load. Taping and triangulation of the floor stations for a second time in 1957 reveal no differences. The close measurements on the "A" pegs also indicate lack of floor heaving since it would in turn affect the angles taken. Visual observations showed no shifting of boulders.

Coordinates of each peg are presented in Table I. The northernmost floor station (F1) was arbitrarily chosen as the reference point and was given a value of 10 m for X', Y', and Z' directions. The coordinate system employed in the tunnel was integrated in 1956 with the main baseline system south of the ice cliff, but the connecting traverse between the two systems could not be re-established in 1957. The 1956 coordinates given in Table I supersedes those presented by Goldthwait*.

MOTION ANALYSIS

The resultant deformation vector was in general directed principally forward (south), slightly downward, and inward to the void. The rate of forward motion increased rapidly upward from the base roughly following a parabolic curve tangent to the floor. Flow of the ice into the tunnel was essentially uniform over the span of the walls with a sharp decrease just above the floor. The downward component of movement was relatively small but erratic over the height of the wall and also decreased abruptly just above the floor. Thus, the basal few centimeters of ice blanketing the subglacial surface had virtually no motion. This fact coincides with observation that lichen on the boulder tops had remained undisturbed by the mobile ice mass. All evidence indicates that deformation proceeded at a uniform rate, and no erratic or backward motions, discontinuities, or significant cracks in the ice were detected.

Forward motion

The forward component of deformation in the tunnel resulted from the longitudinal compressive stress of the advancing ice cap (Fig. 8). Forward motion figures (Table II) were resolved in the actual direction of ice flow as hydrostatic closure deflected longitudinal strain vectors in toward the center of the tunnel. Eliminating the factor of ice creep into the tunnel, absolute forward motion was reduced to a direction approximately 4°W (clockwise) of the +Y' axis and from 4 to 10°E (counterclockwise) of the tunnel axis.

The vertical pattern of forward motion in the absolute plane roughly followed a parabolic curve with the greatest differential strain rates decreasing progressively upward from the base of the glacier (Table III). Movement proceeded in this pattern along each ring on both walls with pegs at comparable height above the floor having the same order of magnitude. A similar type of basal motion has been observed in the deformation of the pit at the inner end of the 1955 tunnel.

Shear strain in the basal few centimeters of the glacier was extremely small as it was only 0.03 mm/m-day at 0.05 m above the bouldery floor. The differential strain over a vertical section rapidly increased to 1.9 mm/m-day at 0.15 m above the floor, and then steadily decreased to 1.0 mm/m-day at 4.40 m above, to 0.5 mm/m-day at 30 m above, and to 0.3 mm/m-day at 40 m above (last two values are cliff face measurements). Thus, on the order to 2% of the forward motion occurred in the lowest 0.4% of the glacier height and 30% forward motion occurred at 10% height. Therefore, most of the gross forward motion near the terminus of this glacier resulted from a shearing action in the lowest portion of the ice mass.

A lateral comparison of forward motion rates at a common height along each wall showed in general less than 5% variation, except at the lower levels. The maximum discrepancy in the "C" pegs was 60%, but in the "B" pegs, which were most irregular, differences reached up to five times the lowest value. The range of values at comparable levels was more divergent along the west wall, largely because ring 4 values were consistently low. Dirt content in the ice at ring 4 was probably a partial retarding influence in the rate of forward motion.

---

* Goldthwait, R. P., Study of ice cliff in Nunatarssuaq, Greenland, U. S. Army Snow Ice and Permafrost Research Establishment, Corps of Engineers, Technical Report 39, 105p., in preparation.

Table I.   Peg and triangulation station coordinates.

Triangulation stations

	X'	Y'	Z'
F1	10.000	10.000	10.000
F2	10.000	11.208	10.005
F3	10.056	12.345	10.109
F4	10.634	15.794	10.243
F5	11.228	19.866	10.484
F6	11.675	23.959	10.704

	1956		Peg coordinates		1957	
	X'	Y'	Z'		X'	Y'	Z'
		Back face				Back face	
B	9.722	9.119	9.999	B	9.771	9.549	10.012
C	9.741	9.245	10.342	C	9.804	9.826	10.337
D	9.715	9.075	10.929	D	9.763	9.694	10.869
E	9.686	8.841	11.548	E	9.785	9.986	11.474
F	9.719	9.116	11.967	F	9.727	9.645	11.881
UW	10.163	9.129	11.917	UW	10.183	9.801	11.790
LW	10.164	9.131	11.182	LW	10.196	9.674	11.100
UE	9.279	9.260	11.862	UE	9.354	10.046	11.727
LE	9.282	9.263	11.246	LE	9.345	9.892	11.104

		Ring 1				Ring 1	
AE	9.121	10.139	9.905	AE	9.133	10.160	9.903
BE	9.048	10.153	10.067	BE	9.132	10.268	10.067
CE	9.017	10.166	10.353	CE	9.136	10.385	-
C'W	10.638	9.936	10.600	C'W	10.531	10.190	-
CW	10.644	9.895	10.437	CW	10.547	10.114	-
B'W	10.634	9.893	10.294	B'W	10.554	10.059	-
BW	10.614	9.897	10.144	BW	10.562	9.991	-
AW	10.571	9.893	10.004	AW	10.567	9.890	-

		Ring 2				Ring 2	
AE	9.677	14.080	10.116	AE	9.689	14.074	10.105
BE	9.574	14.102	10.261	BE	9.637	14.165	10.271
CE	9.458	14.128	10.542	CE	9.615	14.339	10.542
DE	9.497	14.100	11.128	DE	9.775	14.590	11.111
EE	9.428	14.166	12.337	EE	9.680	14.910	12.232
EW	11.320	13.770	12.436	EW	11.142	14.569	12.334
DW	11.314	13.802	11.224	DW	11.090	14.338	11.154
CW	11.345	13.801	10.614	CW	11.193	14.100	10.567
AW	11.187	13.794	10.161	AW	11.179	13.803	10.155
LPW	11.346	13.694	11.428	LPW	11.139	14.489	11.371

Table I (cont'd.)

	1956			Peg coordinates		1957	
	X'	Y'	Z'		X'	Y'	Z'
	Ring 3				Ring 3		
AE	10.091	18.064	10.347	AE	10.095	18.066	10.339
BE	10.070	18.077	10.493	BE	10.113	18.091	10.462
CE	10.961	18.086	10.756	CE	10.220	18.307	10.749
DE	10.069	18.098	11.394	DE	10.312	18.576	11.355
EE	10.046	18.105	12.586	EE	10.356	18.837	12.523
EW	11.609	17.732	12.576	EW	11.381	18.575	12.548
DW	11.518	17.825	11.430	DW	11.314	18.355	11.374
CW	11.493	17.813	10.837	CW	11.363	18.105	10.773
AW	11.447	17.807	10.389	AW	11.445	17.808	10.381
	Ring 4				Ring 4		
AE	10.988	21.946	10.537	AE	10.994	21.947	10.538
BE	10.959	21.952	10.682	BE	11.080	22.063	10.629
CE	10.898	21.958	10.970	CE	11.071	22.165	10.916
DE	10.884	21.974	11.575	DE	11.142	22.463	11.500
EE	10.944	21.988	12.771	EE	11.260	22.772	12.637
FE	10.891	22.011	13.965	FE	11.199	22.936	13.859
YE	11.142	21.962	14.970	YE	11.325	23.230	14.764
YW	12.143	21.756	14.915	YW	12.160	23.040	14.790
HW	12.268	21.725	13.929	HW	12.095	22.654	13.883
G'W	12.250	21.730	13.253	G'W	12.071	22.580	13.222
GW	12.196	21.742	13.064	GW	12.011	22.558	13.035
FW	12.228	21.734	12.742	FW	12.037	22.503	12.715
E'W	12.223	21.724	12.428	E'W	12.029	22.465	12.404
EW	12.240	21.723	12.282	EW	12.050	22.435	12.256
D'W	12.235	21.703	11.614	D'W	12.058	22.156	11.580
DW	12.234	21.702	11.551	DW	12.058	22.148	11.517
CW	12.202	21.697	10.959	CW	12.059	21.883	10.922
BW	12.161	21.695	10.651	BW	12.107	21.776	10.608
AW	12.119	21.708	10.508	AW	12.117	21.705	10.512

Comparison of the over-all absolute motion on each wall shows significant anomalous values at certain lower pegs where small differences became critical (Table II). Differences under about 10% may have resulted from slightly unequal heights, again most prominent down low. Other variations may have been caused by irregularities in bottom topography or, as in ring 4, by dirt layers immediately below pegs.

Closure into tunnel 1

Movement of the tunnel boundaries inward resulted from hydrostatic pressure and longitudinal compressive stress of the moving ice mass applied at an oblique angle to the tunnel axis (Fig. 1-2, 9). Discussion of closure as such must necessarily be limited only to creep rate produced by the load of the overlying ice. Thus, closure figures are given in relation to the distances between the pegs for a common level on the same ring to eliminate the upward increasing effects of forward motion.

The effect of forward motion, causing appreciable increases of closure on the west side, can readily be seen in Figure 9. In comparison to the east side, the west side moved inward at an average of 30% faster at 0.15 m above the floor, 60% at 1.05 m, 120% at 2.25 m, and 230% at 3.40 m.

Table II. Absolute forward motion in a plane 4°E of +Y' axis.

|	Peg	Motion (mm)	Peg	Motion (mm).	% increase	Wall with higher value
Ring 1	AE	20	AW	3		
	BE	120	BW	90	33	East
			B'W	160		
	CE	230	CW	210	10	East
			C'W	250		
Ring 2	AE	*-6	AW	7		.
	BE	60	BW	-		
	CE	220	CW	290	31	West
	DE	510	DW	510	-	-
	EE	760	EW	790	4	West
Ring 3	AE	2	AW	1		
	BE	20	BW	-		
	CE	230	CW	280	22	West
	DE	500	DW	510	2	West
	EE	760	EW	820	8	West
Ring 4	AE	1	AW	*-3		
	BE	120	BW	80	50	East
	CE	210	CW	180	17	East
	DE	510	DW	430	19	East
	EE	800	FW	750	7	East
	FE	940	HW	920	2	East
	YE	1280	YW	1290	1	East

* Minute backward motion included as margin of error.

Table III. Absolute forward motion averages.

Approximate distance (m) above floor	Avg peg	Motion (mm)	Rate (mm/day)	Avg peg	Motion (mm)	Rate (mm/day)	Avg both walls (mm/day)	Differential strain rate above floor (mm/m-day)
0.05	AE	4	0.01	AW	4	0.01	0.01	0.3
0.15	BE	80	0.27	BW	85	0.29	0.28	1.9
0.45	CE	220	0.75	CW	240	0.82	0.79	1.8
1.05	DE	510	1.73	DW	480	1.63	1.68	1.6
2.25	EE	770	2.62	EW	790	2.69	2.66	1.2
3.40	FE	940	3.20	HW	920	3.13	3.17	0.9
4.40	YE	1280	4.35	YW	1290	4.39	4.37	1.0

Table IV. Horizontal closure, ring 4, 1956 tunnel.

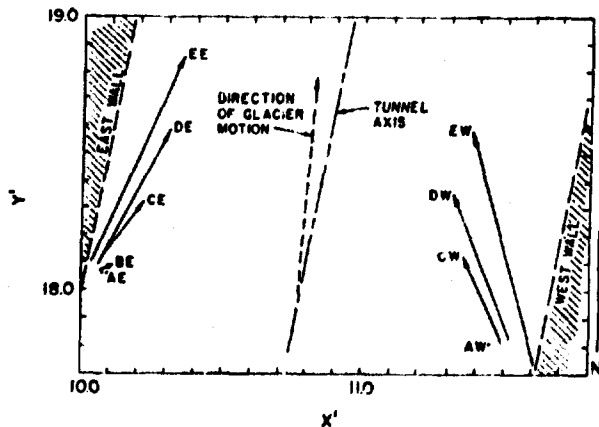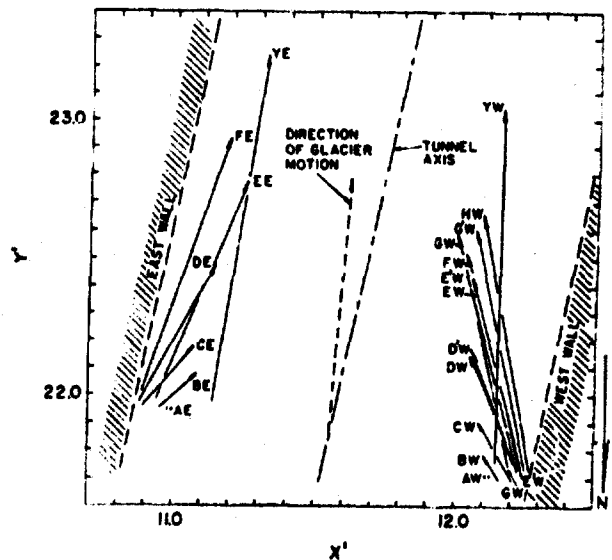|	Dist. above floor (m)	Mid-August 1956 dist. (cm)	Early June 1957 dist. (cm)	Difference (cm)	Rate 294 days (mm/day)
AE - BW	0.05	116	115	1	< 0.01
BE - BW	0.15	124	107	17	0.58
CE - CW	0.45	134	106	28	0.95
DE - DW	1.05	138	96	42	1.43
EE - FW	2.25	131	82	49	1.67
FE - HW	3.40	141	94	47	1.60
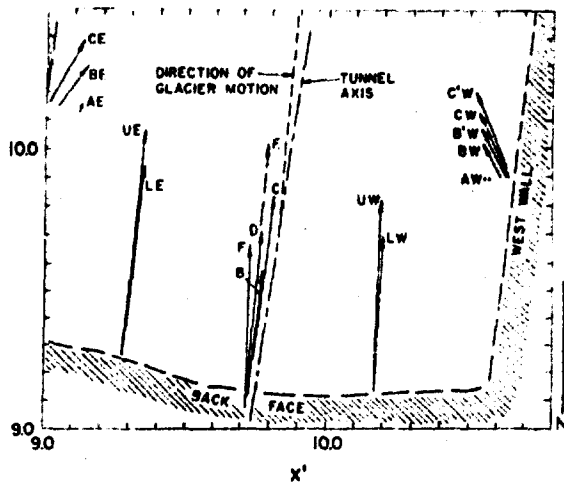
a. Back face and ring 1.
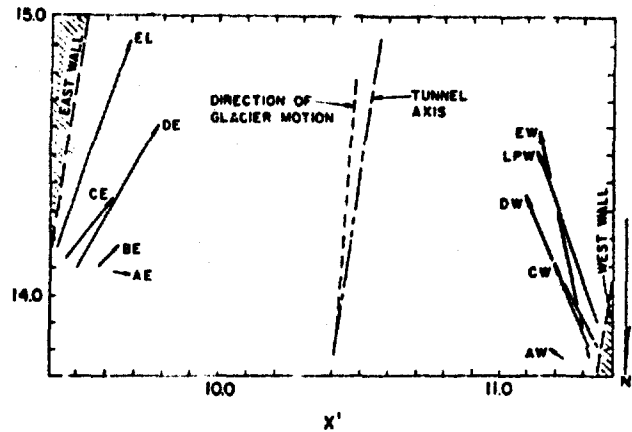
b. Ring 2.

c. Ring 3.

d. Ring 4.

Figure 8. 1956 and 1957 X' and Y' peg coordinates.

The actual rate of approach between pegs of equal height rapidly increased upward to about 1 m above the floor and remained more or less constant above this point (Table IV). Closure at 0.05 m above the floor was almost negligible, less than 0.01 mm/day. At 0.15 m above the floor, closure had greatly increased to 0.58 mm/day and in the next upward 0.30 m it almost doubled to a rate of 0.95 mm/day. The closure rate gradually leveled off so that above 1 m the order of magnitude of closure was under 15% variation.
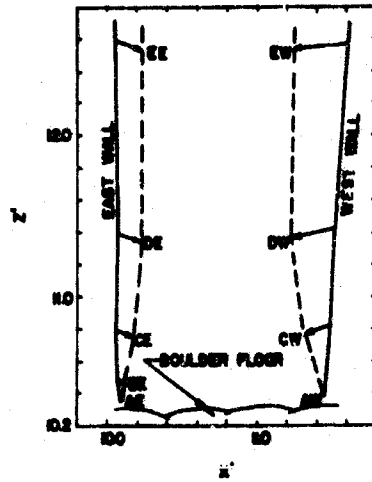
Downward motion

The resultant motion vector was directed slightly downward, although the north dipping ice foliation leads to the suggestion that net ice motion should have been at a gentle upward angle. The component of slump of the walls resulted from gravitational
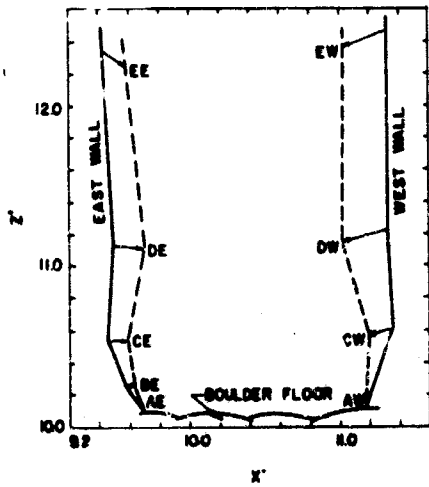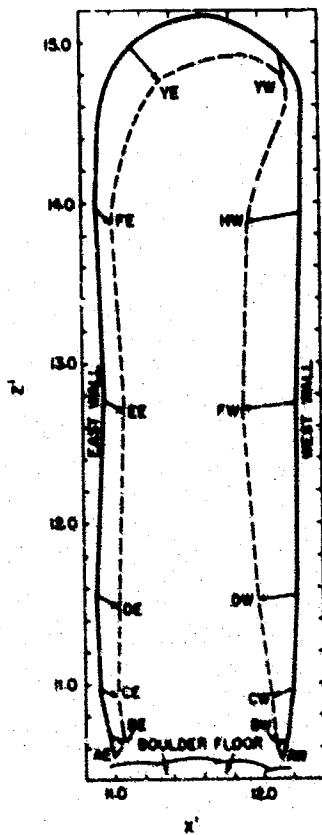
a. Ring 2.

b. Ring 3.

c. Ring 4.

Figure 9.   1956 X' and Z' peg coordinates
and closure vectors normal to tunnel axis.

force acting on the unsupported surface.
This factor probably increased with time
as an overhang developed above the
relatively immobile ice at the glacier
base.

The downward component of motion
was very erratic both in lateral and
vertical relationships (Table V).
At 0.05 m above the floor, the downward
motion was less than 10 mm. At 0.15 m
above, slumping increased rapidly to a
maximum of 50 mm. A significant
correlation between figures of the upper
portion of the wall can not be established
other than to say they were generally
higher than in the lower portion with a
maximum net downward component of
110 mm.

The downward component of the ceiling
arch as recorded on the "Y" pegs of ring 4
was from 130 to 210 mm and resulted from
a combined effect of hydrostatic closure
and slump.

Effect of dirt bands on motion

Several examples provided evidence
that the motion of ice immediately over-
lying dirt layers was retarded (Fig. 3-5).
Peg D'W of ring 4 moved forward slightly
more slowly in relation to the differential
motion of pegs both above and below
(Fig. 7, 8d). In a sequence of pegs shown
in Figure 10, pegs in the ice adjacent to

Table V. Downward component closure.

	Peg	Amount (mm)	Peg	Amount (mm)
Ring 1	AE	0.002		
	BE	0.000		
Ring 2	AE	0.011	AW	0.006
	BE	0.010 *	BW	-
	CE	0.000	CW	0.047
	DE	0.017	DW	0.070
	EE	0.105	EW	0.102
Ring 3	AE	0.008	AW	0.008
	BE	0.031		
	CE	0.037	CW	0.064
	DE	0.039	DW	0.056
	EE	0.063	EW	0.028
Ring 4	AE	0.001 *	AW	0.004 *
	BE	0.053	BW	0.043
	CE	0.054	CW	0.037
	DE	0.075	DW	0.034
	EE	0.084	FW	0.027
	FE	0.106	HW	0.046
	YE	0.206	YW	0.125

* Upward movement.

upper contact of the dirt bands consistently lagged in forward motion. Pegs BW and CW of ring 4 situated directly above dirt layers also moved comparatively slowly.

Core deformation

Cross-sectional shape changes of ice cylinders placed in the west wall of the tunnel were observed. The 10-cm diam cores placed in a hole of the same size in August, 1956, were distorted from the originally circular cross-section to an elliptical cross-section with a corresponding southward tilt (Fig. 11).

Partitions spaced at 90° and composed of cardboard or aluminum foil were set into three of the cores while they were being frozen. The cores were then emplaced in the ice walls with the partitions in essentially horizontal and vertical positions. The vertical dividers tilted southward on the order to 20° while the horizontal partition tilted from 4° southward to 8° northward. A tilt of 34° southward was recorded on a vertical partition of one core but inasmuch as the partition had separated, this value probably was invalid as true tilt.
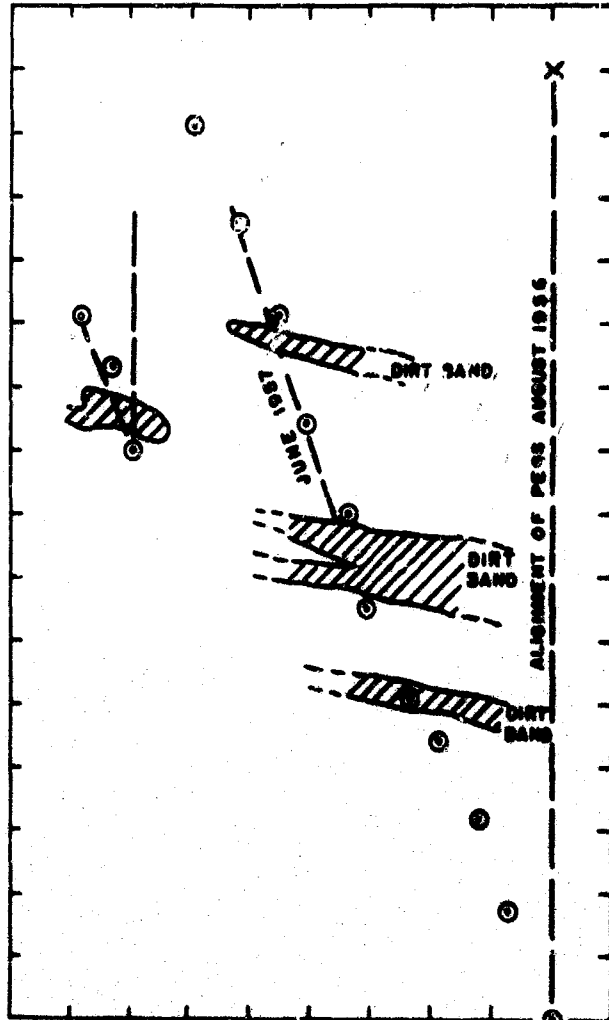

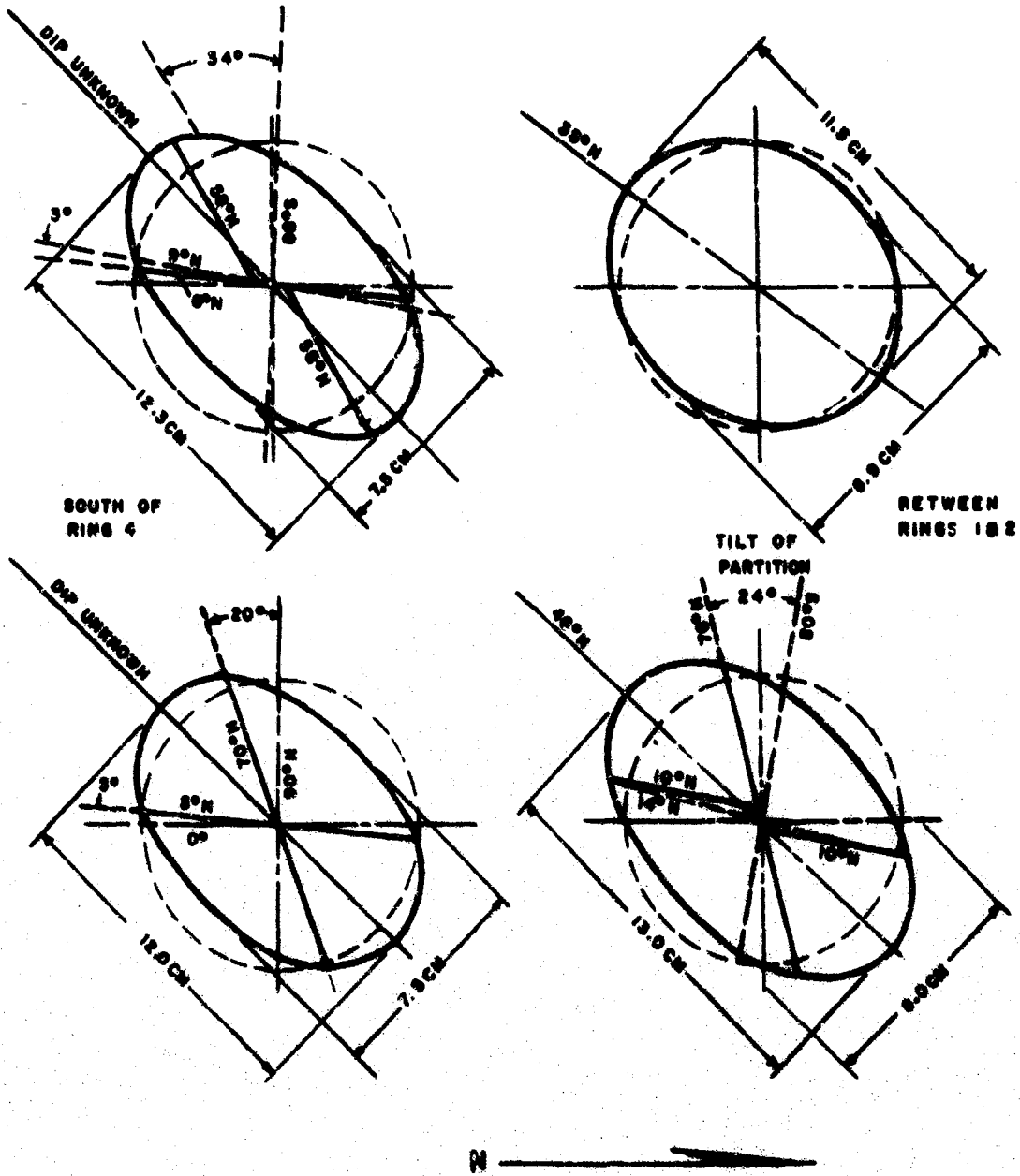Figure 10. Showing tilt and lag of pegs above dirt bands. 1.7 m south of ring 4 on west wall (Fig. 7).

Figure 11. Deformation of cores and tilt of partitions, west wall of tunnel.